Ji-Tuan Feng(冯集团),[1] Yun-Long Liu(刘云龙),[1, a)] Shi-Ping Wang(王诗平),[1] Shuai Zhang(张帅),[1,2] and Longbin Tao(陶龙宾)[3]

[1)] *College of Shipbuilding Engineering Harbin Engineering University Harbin 150001 China*

[2)] *Nanhai Institute of Harbin Engineering University Sanya 572024 China*

[3)] *Department of Naval Architecture Ocean and Marine Engineering University of Strathclyde Glasgow G4 0LZ United Kingdom*

1–8 9–13

14–16 17–19

20–27

28–32

33–47 48

49

50

33,34

36

37

[a)] Corresponding author: yunlong_liu@hrbeu.edu.cn

This is a peer-reviewed, accepted author manuscript of the following article: Feng, J. T., Liu, Y. L., Wang, S. P., Zhang, S., & Tao, L. (2023). Numerical analysis of nonlinear interaction between a gas bubble and free surface in a viscous compressible liquid. Physics of Fluids, 35(7), [072103]. https://doi.org/10.1063/5.0147605

42

51–55

56

57 58

54

53

38

45

39

40

41

59

[60]

$\times$

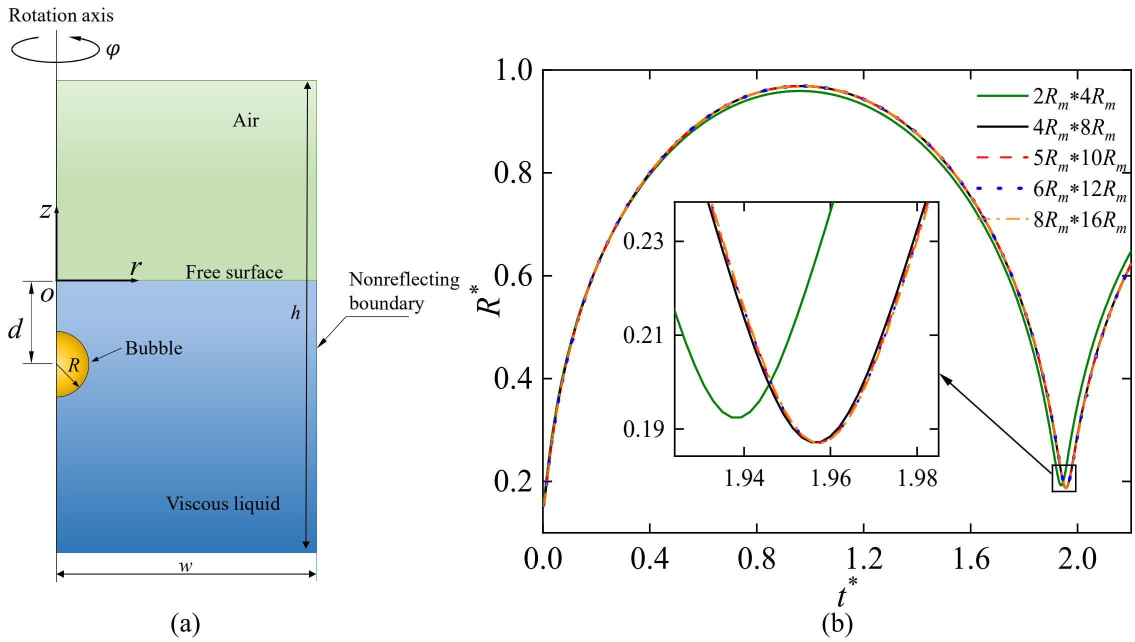

$\times$ $\times$ $\times$ $\times$ $\times$

[34,61–64]

$$\nabla\cdot \quad \boldsymbol{v} \qquad \nabla\cdot\boldsymbol{v}$$
$$\nabla\cdot \quad \boldsymbol{v}$$
$$\bar{\boldsymbol{v}} \quad \nabla\cdot\bar{\boldsymbol{v}}\otimes\boldsymbol{v} \quad \bar{\boldsymbol{v}} \quad \nabla \quad \bar{\mathbf{g}} \quad \nabla\cdot\boldsymbol{\tau} \quad \boldsymbol{\tau}$$
$$\nabla\cdot \quad \boldsymbol{v} \qquad \nabla\cdot\boldsymbol{v}$$

$\sum$ $\boldsymbol{v}$ $\mathbf{g}$ $\boldsymbol{\tau}$ $\boldsymbol{\tau}$ $\boldsymbol{\tau}$ $\otimes$ ∇

$\boldsymbol{\tau}$ [38]

$$\begin{cases} \boldsymbol{\tau} \quad \boldsymbol{\tau} \quad \left[\nabla \boldsymbol{v} \quad \nabla \boldsymbol{v} \quad - - \left(\nabla \cdot \boldsymbol{v} \quad -\right) \mathbf{I}\right] \\ \left[\; - - - \left(\nabla \cdot \boldsymbol{v} \quad -\right)\right] \end{cases}$$

$\mathbf{I}$

$\boldsymbol{\tau} \quad \nabla \boldsymbol{v}$

[65]

$- \quad -$

$3 \quad 3$

[66–69]

[60,62,66,70,71]

$$\iint_{\Omega} - \frac{\boldsymbol{v}}{} \qquad \iint_{\Omega} \left(\nabla \quad - \mathbf{g} \; - \boldsymbol{\tau} \cdot \nabla \quad \frac{\boldsymbol{\tau}}{} \right) \; - \int_{\Omega} \quad \boldsymbol{n} \qquad \int_{\Omega} \boldsymbol{\tau} \quad \cdot \boldsymbol{n}$$

$\boldsymbol{n}$

$$\mathbf{M}\mathbf{A}_{\text{node}} \quad \mathbf{F}_{\text{node}}$$

$\mathbf{M} \quad \iint_{\Omega} -$ $\quad \mathbf{A}_{\text{node}} \quad \mathbf{F}_{\text{node}}$

[67]

$$\boldsymbol{v}^{\;+1\;\;2} \quad \boldsymbol{v}^{\;-1\;\;2} \quad \boldsymbol{a}$$

$$\boldsymbol{x}^{\;+1} \quad \boldsymbol{x} \quad \boldsymbol{v}^{\;+1\;\;2}$$

$\boldsymbol{a}$

$$\begin{cases} \nabla \cdot \boldsymbol{v} \quad \nabla \cdot \boldsymbol{v} \\ \nabla \cdot \boldsymbol{v} \\ \left(\quad \right) \nabla \cdot \boldsymbol{v} \end{cases}$$

[72]

[73] [66,72]

$$|\boldsymbol{v}|$$

[66]

2

0 0 atm

$_{\mathrm{atm}} \quad |\mathbf{g}|$

∞ $*$

$*$ $1 \;\; 2$

$*$

$\sqrt{}$	$\sqrt{}$	

^{2}				
$\|\mathbf{g}\|$	$_0$		$\sqrt{}$ ∞	$\sqrt{}$

$\times$ $\times$ $\times$ $\times$ $\times$

$\times$

$\times$

$\times$

[50]

$$\left(\quad\right)\left[\frac{^2}{}\left(- \;^2 \; -\boldsymbol{v}^2 \quad \right)\right] \quad ^2 \quad ^2$$

$$\boldsymbol{v} \quad \boldsymbol{v} - \mathbf{g} - \boldsymbol{v}$$

$\boldsymbol{v}$

$\cdot$ $\cdot$ $|\cdot|$

[49]

[74]

$\approx$ $|\mathbf{g}|$ ^{2}

[2]

$^*_0$ [50]

∞

20230410

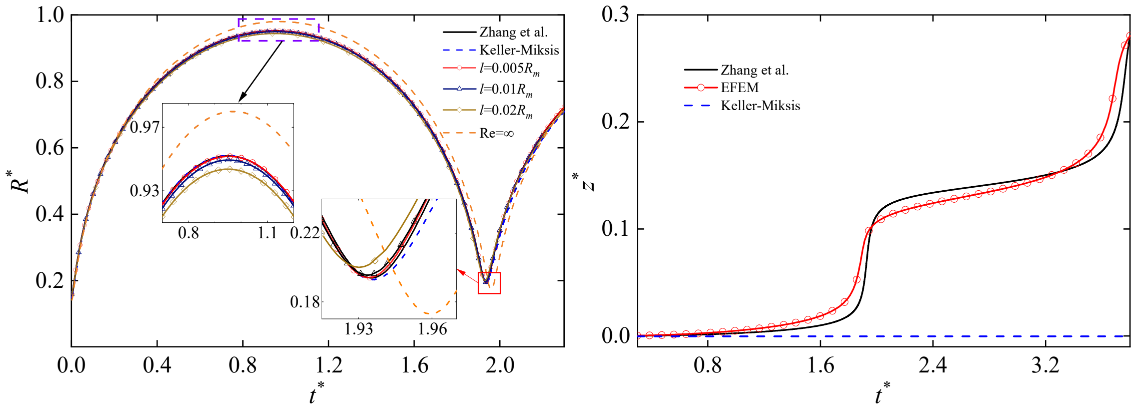

(a) (b)

3

. ○

∞ 50 ∞

∞

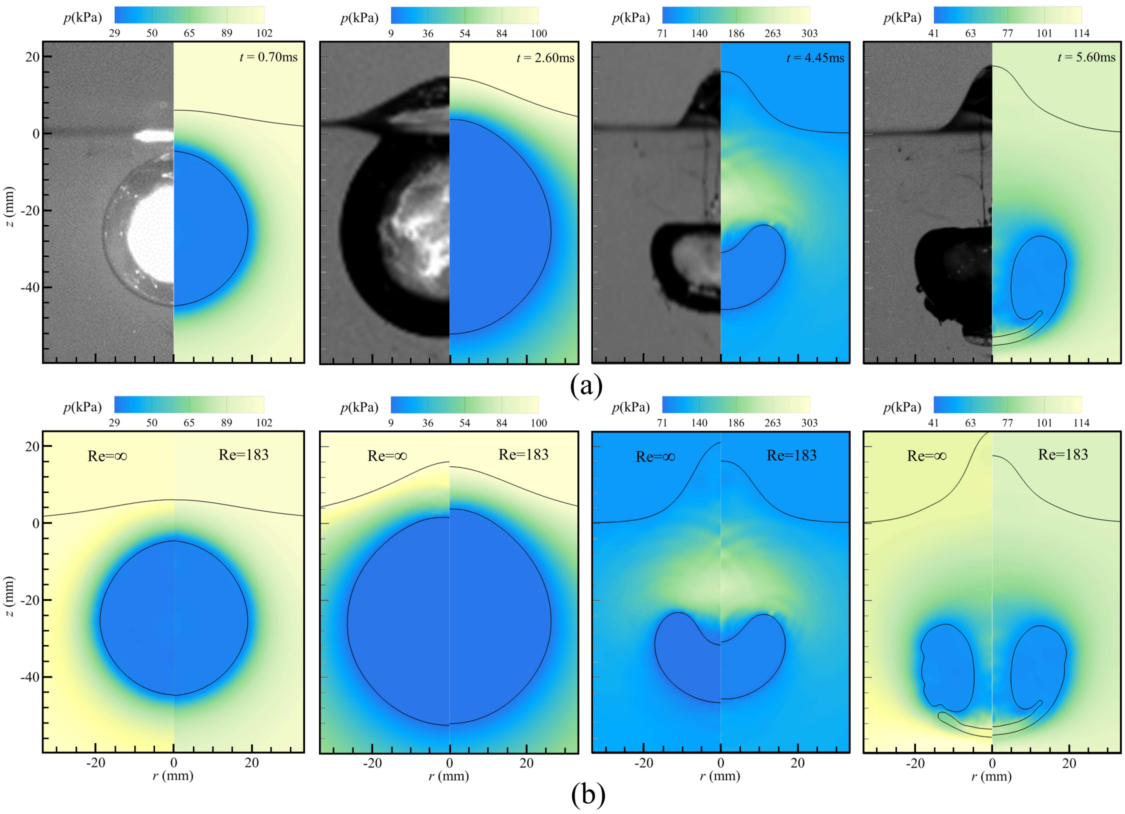

$^{*}_{0}$

$\times$

∞

∞

∞

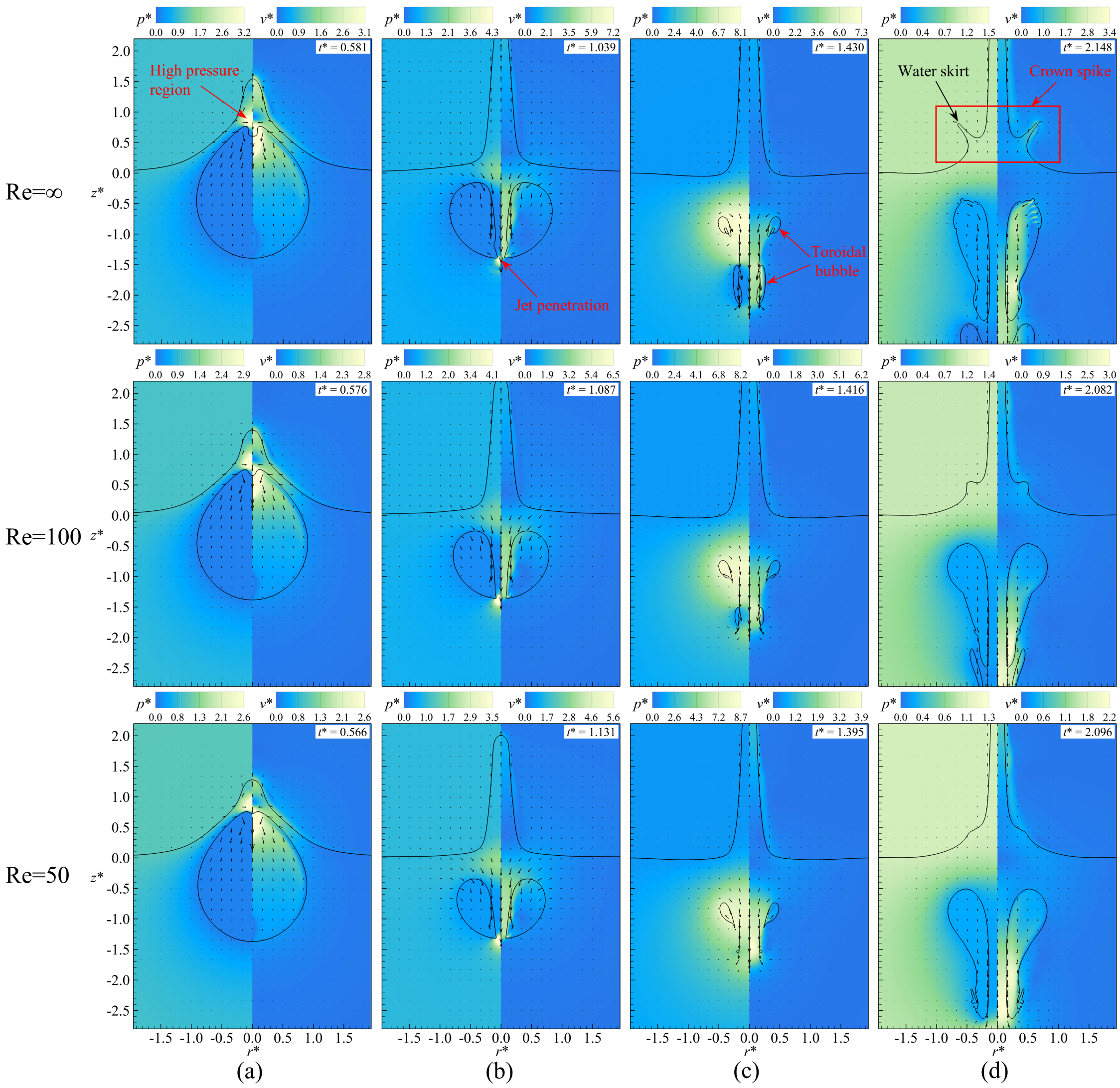
Re=∞
Re=100
Re=50
High pressure region
Jet penetration
Toroidal bubble
Water skirt
Crown spike
t* = 0.581
t* = 1.039
t* = 1.430
t* = 2.148
t* = 0.576
t* = 1.087
t* = 1.416
t* = 2.082
t* = 0.566
t* = 1.131
t* = 1.395
t* = 2.096
(a)
(b)
(c)
(d)

∞

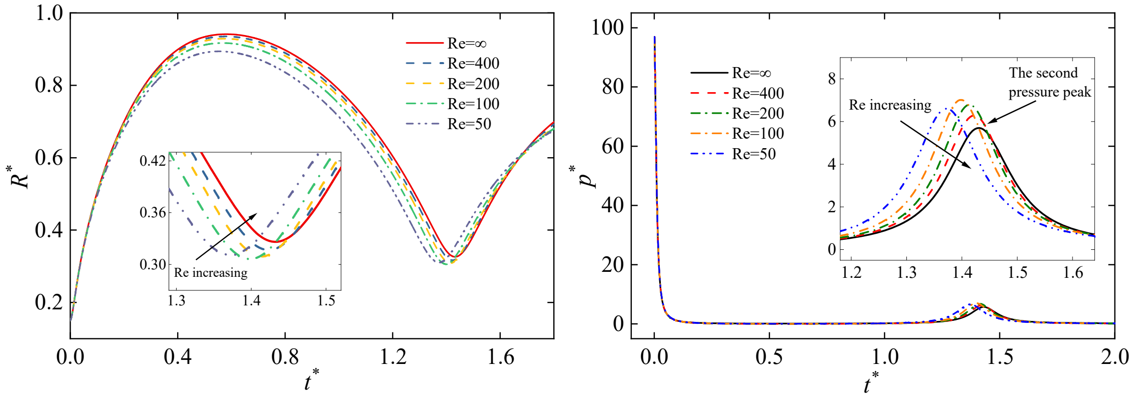
Re=∞
Re=400
Re=200
Re=100
Re=50
Re increasing
R*
t*
Re increasing
The second pressure peak
p*
t*
(a) (b)

∞

*

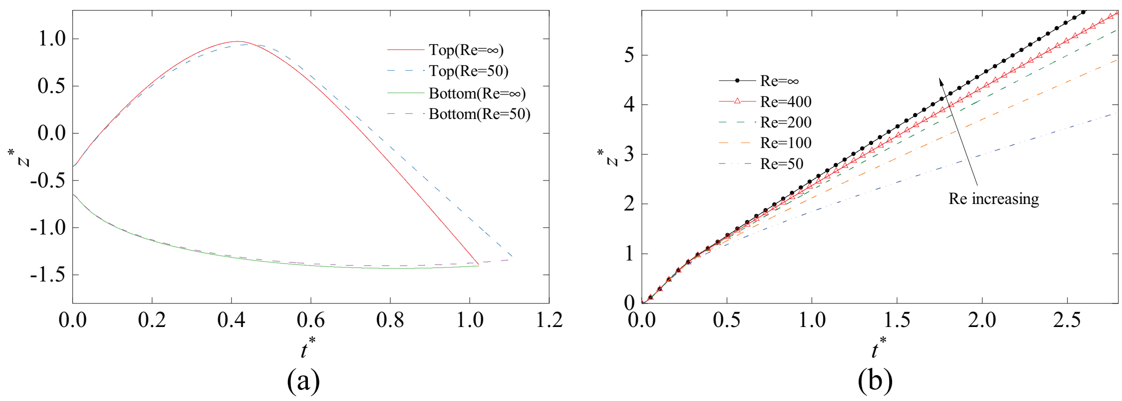

FIG. 6. Time histories of (a)the bubble top and bottom locations at $\mathrm{Re} = \infty$ and 50, $\gamma_d = 0.5$; (b)the free surface spike height at different Reynolds numbers $\mathrm{Re} = 50, 100, 200, 400, \infty$, and stand-off parameter $\gamma_d = 0.5$, respectively.

violently affected by the high-pressure region than the bottom. The jet penetrates the bottom at about $t^* = 1.03$, while the $\mathrm{Re} = 50$ bubble jet penetrates at $t^* = 1.13$. The slope of the displacement curve of the bubble in Fig.6(a) represents the jet velocity. It can be found that compared with the bubble with $\mathrm{Re} = 50$, the jet velocity is faster without considering the viscosity of the liquid. Meanwhile, compared with Fig.4(a), it can also be found that the inviscid bubble has formed an obvious top jet before the bubble reaches the maximum volume.

The evolution of the free surface spike height at different Reynolds numbers is shown in Fig.6(b). In the initial expansion stage of the bubble, due to the relatively long distance from the free surface, the change of the free surface with different Re is the same. It can be seen from Fig.6(b) that as the Re decreases, the viscous effect increases and the height of the jet on the free surface decreases significantly. The main reason is the significant rate of change of tangential velocity caused by the jet, which leads to sizeable viscous friction and faster kinetic energy loss.

The pulsation of the bubble in the second period induces a low axisymmetric water skirt on both sides of the free-surface jet, called the crown spike. Fig.7(a) shows the shape of the crown spike under different Reynolds numbers Re when the bubble expands to the maximum volume in the second pulsation cycle. With the increase in Reynolds number, the phenomenon of a crown spike is more pronounced, and the height of the water skirt is also increasing. And the shape is sharp, and when $\mathrm{Re} = 50$, the free surface almost does not form a crown spike, indicating that the viscous effect weakens the evolution of the free surface. Fig.7(b) shows the shapes of bubbles when jet impact with different Reynolds numbers. The $\mathrm{Re} = \infty$ bubble jet has a bulge at the front, called a mushroom-shaped jet. Koukouvinis[26] believes that the jet is caused by interface instability. However, compared with an inviscid bubble, the jet tip at the top of low Reynolds number bubbles is smoother, and no mushroom-shaped jet appears. Meanwhile, the volume of jet penetration is smaller, and the velocity and impact strength of the bubble jet is weak, which is reflected in the contours in Fig.4.

The bubble expands under the initial pressure. With the increase of liquid viscosity, the Reynolds number under the corresponding conditions decreases. The retardation effect of viscosity on bubble expansion becomes stronger and stronger, and the maximum radius of the bubble decreases. At the same time, the bubble jet is also affected by the viscosity, the jet velocity decreases with the decrease of the Reynolds number, and the jet penetration time is also delayed. The viscosity of the liquid affects the height and speed of the free surface jet: the viscosity increases, and the speed and height of the free surface jet decrease. When the viscosity increases to a specific value, the free surface crown spike generated by the pulsation of the bubbles will disappear, and the viscosity of the liquid weakens the interaction between bubbles and the free surface.

B. Bubble dynamics with different stand-off parameters

In the same fluid, the viscosity coefficient of the liquid has been determined. When a pulsating bubble is generated using the same method, the effect of viscosity on bubbles is unchanged. The parameter that affects the dynamics of bubbles and the free surface is the distance d (as shown in Fig.1(a)), and the dimensionless parameter γ_d represents the inception depth of the bubble. Set $\mathrm{Re} = 100$, other parameters remain the same

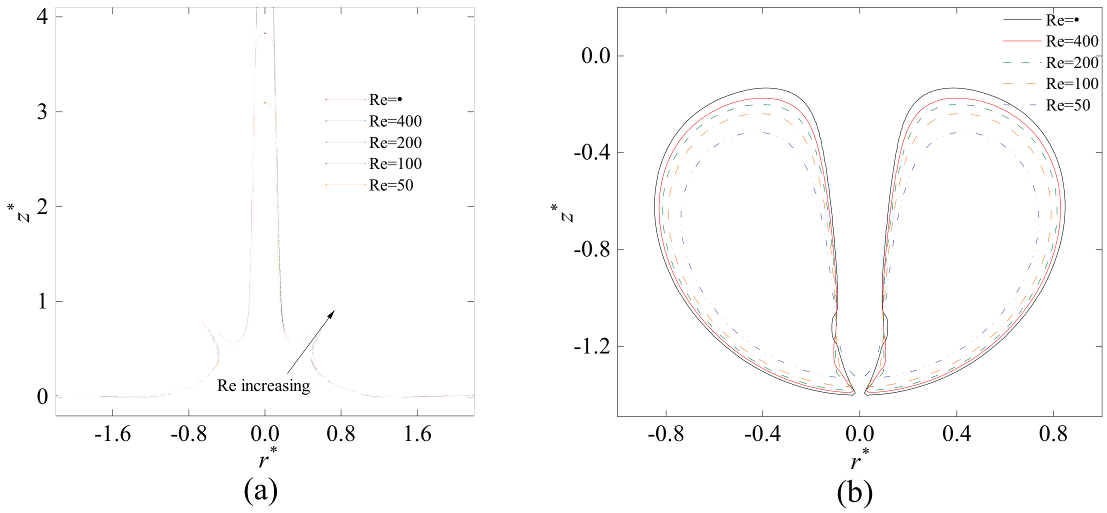

FIG. 7. (a)Shape of the free surface; (b)shape of the bubble when the jet impact at different Reynolds numbers $\mathrm{Re} = 50, 100, 200, 400, \infty$, and stand-off parameter $\gamma_d = 0.5$, respectively.

as the previous section, and study the bubble dynamics for $\gamma_d = 0.5 - 1.5$.

Fig.8 shows the bubble and the free surface shapes, pressure, and velocity contours at three important moments when Reynolds number $\mathrm{Re} = 100$ and stand-off parameter $\gamma_d = 0.5$, 1.0 and 1.5, respectively, corresponding to maximum bubble volume, jet impact, and maximum volume in the second pulsation period. The dimensionless time for the bubble to expand to the maximum radius increases with γ_d, $t^* = 0.576$, 0.775, and 0.848, respectively, as shown in Fig.8. The bubble jet is already formed in the expansion phase when $\gamma_d = 0.5$, while the bubble jet in the other two cases starts to form in the contraction phase. Compared with the other two conditions, the bubble and the free surface jet with smaller γ_d are also more slender, and the jet impacts the bottom earlier. As shown in Fig.8(b), bubble jets of $\gamma_d = 1.0$ and 1.5 impacting the bottom occurred near the moment when bubbles collapsed to the minimum volume. In contrast, bubble jets of $\gamma_d = 0.5$ had penetrated through the bottom in the contraction stage, and a local high-pressure region was formed when the jets penetrated through the bottom. It can be seen from Fig.8(c) that the bubble with $\gamma_d = 0.5$ produces toroidal splitting because the jet penetrates the bottom earlier, and the annular sideways jet is generated when the bubble continues to collapse. This phenomenon is noticeable at large Reynolds numbers, and bubbles with larger stand-off parameters do not produce apparent toroidal splitting. At the same time, with the increase of γ_d, the free surface jet becomes lower, and the phenomenon of a crown spike is less obvious. The free surface does not produce a crown spike during the secondary pulsation of the bubble when $\gamma_d = 1.5$.

Fig.9(a) shows the shape of the bubble when the jet penetrates with different γ_d. It can be seen from the figure that with the increase of the stand-off parameter, the volume of bubble jet impact continues to decrease. When the inception depth is small, the impact time of the jet is earlier than the minimum volume time due to the strong interaction between bubbles and the free surface. The bubble jet width also varies with the change of the stand-off parameter. When the γ_d increases from 0.5 to 1.0, the jet width gradually increases; when the γ_d increases from 1.0 to 1.5, the jet width gradually decreases, which is the same as the law obtained by Li[38] without considering viscosity. With the increase of γ_d, the water jet penetration time is delayed, and the jet width changes due to the different degrees of bubble shrinkage. It can also be seen from the velocity contours in Fig.8(b) that the velocity of the jet impinges increases with the increase of γ_d. Fig.9(b) shows the shape of the free surface when the jet penetrates. With the increase of γ_d, the jet height of the free surface decreases while the jet width gradually increases. From the pressure contours in Fig.8(a), there is no high-pressure region below the free surface when the γ_d is large, which is not conducive to the generation of the bubble and the free surface jet. At the same time, the effect of bubble expansion on the free surface is weakened, which is also the reason for the low height of the free surface jet. Fig.10 shows the position changes of the top and bottom of the bubble on the axis, which can vividly see the changing trend of the axial length of the bubble. Meanwhile, the velocity of the bubble surface at the axis can also be obtained by calculating the slope of the curve. In the early stage of bubble expansion, the displacement of the upper surface of bubbles with different γ_d is different, and the displacement decreases with the increase

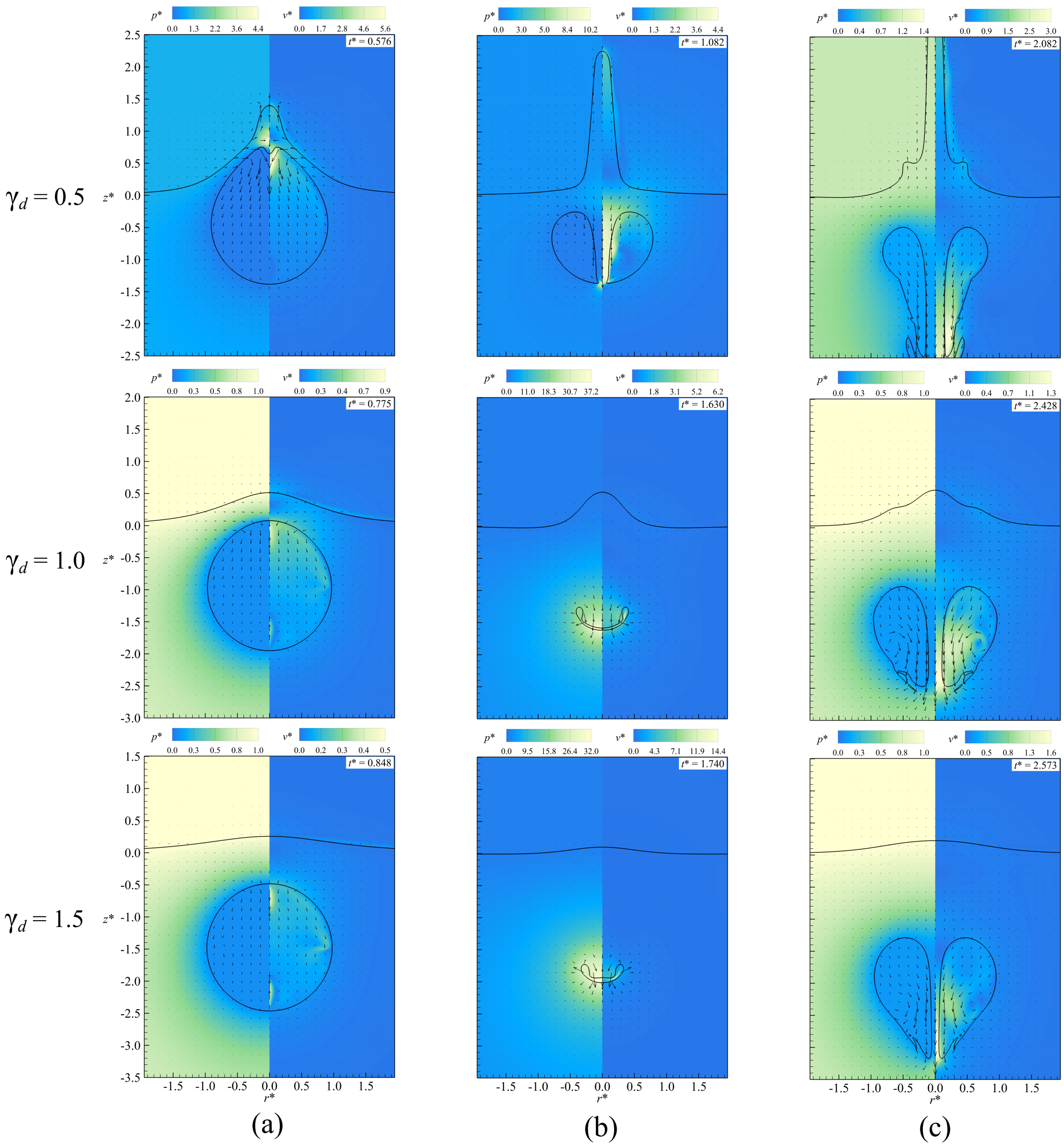
γd = 0.5
γd = 1.0
γd = 1.5
(a)
(b)
(c)

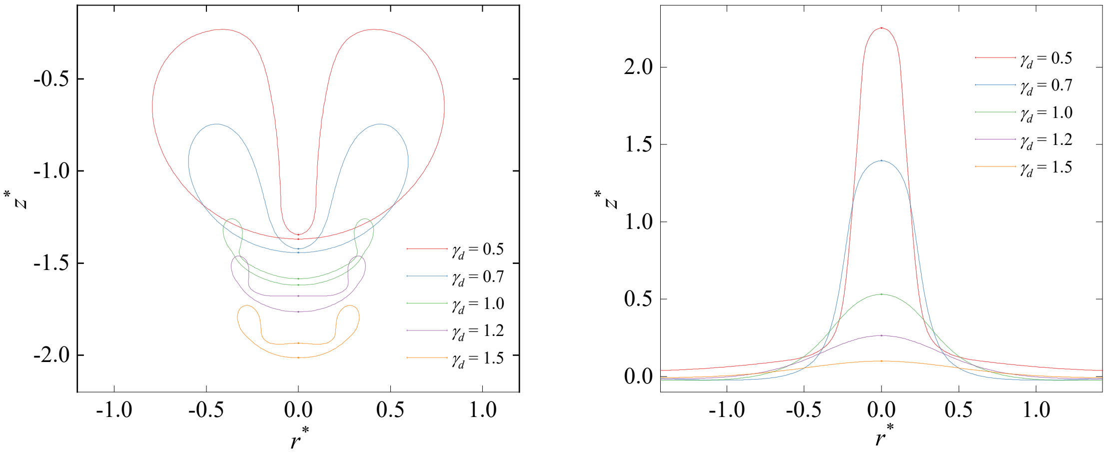
-0.5
-1.0
-1.5
-2.0
z^*
-1.0 -0.5 0.0 0.5 1.0
r^*
$\gamma_d = 0.5$
$\gamma_d = 0.7$
$\gamma_d = 1.0$
$\gamma_d = 1.2$
$\gamma_d = 1.5$
2.0
1.5
1.0
0.5
0.0

(a) (b)

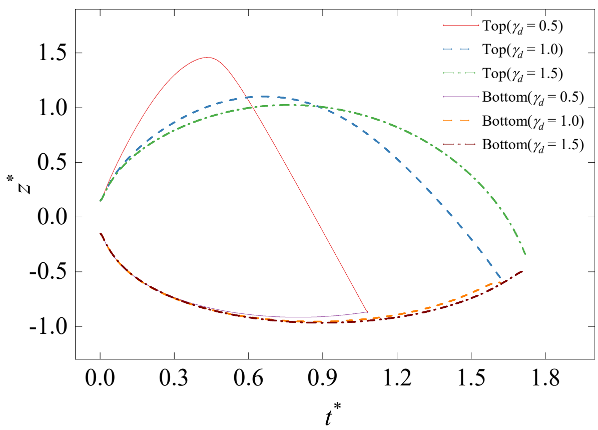
1.5
1.0
0.5
0.0
-0.5
-1.0
z^*
0.0 0.3 0.6 0.9 1.2 1.5 1.8
t^*
Top($\gamma_d = 0.5$)
Top($\gamma_d = 1.0$)
Top($\gamma_d = 1.5$)
Bottom($\gamma_d = 0.5$)
Bottom($\gamma_d = 1.0$)
Bottom($\gamma_d = 1.5$)

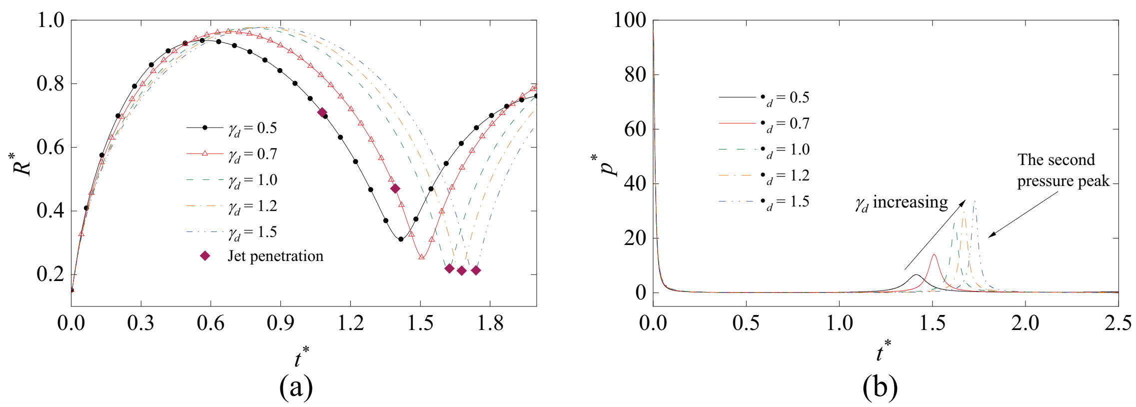

FIG. 11. Time histories of (a)the equivalent radius of bubbles; (b)average pressure in bubbles with different stand-off parameters γ_d=0.5, 0.7, 1.0, 1.2, and 1.5, Re=100, respectively.

(I) As Re decreases, the bubble oscillation amplitude and period decrease, the bubble jet shape is blunter, the jet velocity decrease, and the impact time is delayed. At a lower Re, the jet is weaker and associated with less kinetic energy, resulting in earlier collapse. The viscosity also reduces the toroidal bubble splitting during pulsation, and the bubble with Re=50 hardly splits.

(II) As γ_d increases, the maximum bubble volume increases, the minimum bubble volume decreases, and the second pressure peak of the bubble increases. When γ_d decreases from 1.5 to 0.5, the jet becomes sharper and impacts the opposite bubble surface earlier.

(III) As Re decreases, the height and velocity of the free surface jet decrease, and the crown spike height decreases or even disappears in the second pulsation cycle. As γ_d increases, the free surface jet's height decreases, the jet's width increases, and the crown spike tends to be low or even disappear.

ACKNOWLEDGMENTS

The authors would like to acknowledge support from the Finance Science and Technology Project of Hainan Province (Grant No. ZDKJ2021020), the National Natural Science Foundation of China (Grant Nos. 52088102 and 51909041), the Natural Science Foundation of Heilongjiang Province of China(No. YQ2021E012) and Development Program(JCKY2021604B027). Thanks to Dr. Hao Tang for his help in the data analysis of this paper.

[1]A. M. Zhang, W. B. Wu, Y. L. Liu, and Q. X. Wang, "Nonlinear interaction between underwater explosion bubble and structure based on fully coupled model," Physics of Fluids **29**, 082111 (2017).
[2]E. Klaseboer, K. C. Hung, C. Wang, C. W. Wang, B. C. Khoo, P. Boyce, S. Debono, and H. Charlier, "Experimental and numerical investigation of the dynamics of an underwater explosion bubble near a resilient/rigid structure," Journal of Fluid Mechanics **537**, 387–413 (2005).
[3]X. L. Yao, A. M. Zhang, and Y. C. Liu, "Interaction of two three-dimensional explosion bubbles," Journal of Marine Science and Application **6**, 7 (2007).
[4]A. M. Zhang and Y. L. Liu, "Improved three-dimensional bubble dynamics model based on boundary element method," Journal of Computational Physics **294**, 208–223 (2015).
[5]A. Tatlısuluoğlu and S. Beji, "Blast pressure measurements of an underwater detonation in the sea," Journal of Marine Science and Application , 1–8 (2021).
[6]N. Zhang, Z. Zong, and W. P. Zhang, "Dynamic response of a surface ship structure subjected to an underwater explosion bubble," Marine Structures **35**, 26–44 (2014).
[7]G. Li, D. Shi, L. Wang, and K. Zhao, "Measurement technology of underwater explosion load: A review," Ocean Engineering **254**, 111383 (2022).
[8]S. S. Emamzadeh, "Nonlinear dynamic response of a fixed offshore platform subjected to underwater explosion at different distances," Journal of Marine Science and Application **21**, 168–176 (2022).
[9]Q. X. Wang and K. Manmi, "Three dimensional microbubble dynamics near a wall subject to high intensity ultrasound," Physics of Fluids **26**, 032104 (2014).
[10]H. Lais, P. S. Lowe, T. H. Gan, and L. C. Wrobel, "Numerical modelling of acoustic pressure fields to optimize the ultrasonic cleaning technique for cylinders," Ultrasonics Sonochemistry **45**, 7–16 (2018).
[11]W. D. Song, M. H. Hong, B. Lukyanchuk, and T. C. Chong, "Laser-induced cavitation bubbles for cleaning of solid surfaces," Journal of Applied Physics **95**, 2952–2956 (2004).

[12]D. S. Fatyukhin, R. I. Nigmetzyanov, V. M. Prikhodko, A. V. Sukhov, and S. K. Sundukov, “A comparison of the effects of ultrasonic cavitation on the surfaces of 45 and 40kh steels,” Metals **12**, 138 (2022).
[13]J. Mustonen, O. Tommiska, A. Holmström, T. Rauhala, P. Moilanen, M. Gritsevich, A. Salmi, and E. Hæggström, “Fem-based time-reversal enhanced ultrasonic cleaning,” Ultrasonics Sonochemistry **79**, 105798 (2021).
[14]E. Stride and N. S. Ari, “Microbubble ultrasound contrast agents: a review,” Proceedings of the Institution of Mechanical Engineers Part H Journal of Engineering in Medicine **217**, 429–47 (2003).
[15]P. G. Durham and P. A. Dayton, “Applications of sub-micron low-boiling point phase change contrast agents for ultrasound imaging and therapy,” Current Opinion in Colloid & Interface Science **56**, 101498 (2021).
[16]H. Yusefi and B. Helfield, “Ultrasound contrast imaging: Fundamentals and emerging technology,” Frontiers in Physics , 100 (2022).
[17]C. B. Arnold, P. Serra, and A. Piqué, “Laser direct-write techniques for printing of complex materials,” Mrs Bulletin **32**, 23–31 (2007).
[18]M. Jalaal, M. K. Schaarsberg, C.-W. Visser, and D. Lohse, “Laser-induced forward transfer of viscoplastic fluids,” Journal of fluid mechanics **880**, 497–513 (2019).
[19]P. Serra and A. Piqué, “Laser-induced forward transfer: fundamentals and applications,” Advanced Materials Technologies **4**, 1800099 (2019).
[20]R. N. Cui, S. Li, S. P. Wang, and A. M. Zhang, “Pulsating bubbles dynamics near a concave surface,” Ocean Engineering **250**, 110989 (2022).
[21]Q. X. Wang, “Non-spherical bubble dynamics of underwater explosions in a compressible fluid,” Physics of Fluids **25**, 072104 (2013).
[22]A. M. Zhang, P. Cui, J. Cui, and Q. X. Wang, “Experimental study on bubble dynamics subject to buoyancy,” Journal of Fluid Mechanics **776**, 137–160 (2015).
[23]P. Koukouvinis, M. Gavaises, O. Supponen, and M. Farhat, “Numerical simulation of a collapsing bubble subject to gravity,” Physics of Fluids **28**, 032110 (2016).
[24]S. Li, B. C. Khoo, A. M. Zhang, and S. P. Wang, “Bubble-sphere interaction beneath a free surface,” Ocean Engineering **169**, 469–483 (2018).
[25]L. T. Liu, X. L. Yao, A. M. Zhang, and Y. Y. Chen, “Numerical analysis of the jet stage of bubble near a solid wall using a front tracking method,” Physics of Fluids **29**, 012105 (2017).
[26]P. Koukouvinis, M. Gavaises, O. Supponen, and M. Farhat, “Simulation of bubble expansion and collapse in the vicinity of a free surface,” Physics of Fluids **28**, 052103 (2016).
[27]A.-M. Zhang, S.-M. Li, P. Cui, S. Li, and Y.-L. Liu, “Interactions between a central bubble and a surrounding bubble cluster,” Theoretical and Applied Mechanics Letters , 100438 (2023).
[28]L. Liu, J. Wang, and K. Tang, “Coupling characteristics of bubbles with a free surface initially disturbed by water waves,” Physics of Fluids **34**, 042117 (2022).
[29]A. Pearson, E. Cox, J. R. Blake, and S. R. Otto, “Bubble interactions near a free surface,” Engineering Analysis with Boundary Elements **28**, 295–313 (2004).
[30]Q. Wang, K. Yeo, B. Khoo, and K. Lam, “Nonlinear interaction between gas bubble and free surface,” Computers & fluids **25**, 607–628 (1996).
[31]Y. L. Liu, Q. X. Wang, S. P. Wang, and A. M. Zhang, “The motion of a 3d toroidal bubble and its interaction with a free surface near an inclined boundary,” Physics of Fluids **28**, 122101 (2016).
[32]Y. Sun, Z. Yao, H. Wen, Q. Zhong, and F. Wang, “Cavitation bubble collapse in a vicinity of a rigid wall with a gas entrapping hole,” Physics of Fluids **34**, 073314 (2022).
[33]J. R. Blake and D. C. Gibson, “Growth and collapse of a vapour cavity near a free surface,” J. Fluid Mech. **111**, 123–123 (1981).
[34]J. R. Blake and D. C. Gibson, “Cavitation bubbles near boundaries,” Annual Review of Fluid Mechanics **19**, 99–123 (1987).
[35]J. Li and J. L. Rong, “Bubble and free surface dynamics in shallow underwater explosion,” Ocean Engineering **38**, 1861–1868 (2011).
[36]O. Supponen, D. Obreschkow, M. Tinguely, P. Kobel, N. Dorsaz, and M. Farhat, “Scaling laws for jets of single cavitation bubbles,” Journal of Fluid Mechanics **802**, 263–293 (2016).
[37]S. Zhang, S. Wang, and A. Zhang, “Experimental study on the interaction between bubble and free surface using a high-voltage spark generator,” Physics of Fluids **28**, 032109 (2016).
[38]T. Li, A. M. Zhang, S. P. Wang, S. Li, and W. T. Liu, “Bubble interactions and bursting behaviors near a free surface,” Physics of Fluids **31**, 042104 (2019).
[39]L. T. Liu, X. B. Chen, W. Q. Zhang, and A. M. Zhang, “Study on the transient characteristics of pulsation bubble near a free surface based on finite volume method and front tracking method,” Physics of Fluids **32**, 052107 (2020).
[40]Y. Saade, M. Jalaal, A. Prosperetti, and D. Lohse, “Crown formation from a cavitating bubble close to a free surface,” Journal of Fluid Mechanics **926** (2021).
[41]N. Bempedelis, J. Zhou, M. Andersson, and Y. Ventikos, “Numerical and experimental investigation into the dynamics of a bubble-free-surface system,” Physical Review Fluids **6**, 013606 (2021).
[42]R. T. Cerbus, H. Chraibi, M. Tondusson, S. Petit, D. Soto, R. Devillard, J. P. Delville, and H. Kellay, “Experimental and numerical study of laser-induced secondary jetting,” Journal of Fluid Mechanics **934** (2022).
[43]T.-H. Phan, V.-T. Nguyen, and W.-G. Park, “Numerical study on strong nonlinear interactions between spark-generated underwater explosion bubbles and a free surface,” International Journal of Heat and Mass Transfer **163**, 120506 (2020).
[44]S.-M. Li, A.-M. Zhang, and N.-N. Liu, “Effect of a rigid structure on the dynamics of a bubble beneath the free surface,” Theoretical and Applied Mechanics Letters **11**, 100311 (2021).
[45]D. Singh and A. K. Das, “Dynamics of inner gas during the bursting of a bubble at the free surface,” Physics of Fluids **33** (2021), 052105.
[46]Q. Wang, W. Liu, C. Corbett, and W. R. Smith, “Microbubble dynamics in a viscous compressible liquid subject to ultrasound,” Physics of fluids , 34 (2022).

[47]Z. Wang, R. Duan, L. Liu, and H. Yang, "Jetting behavior as a bubble bursts in free space," Physics of Fluids **33**, 023304 (2021).
[48]M. S. Plesset, "The dynamics of cavitation bubbles," J.appl.mech **16**, 277–282 (1949).
[49]J. B. Keller and M. Miksis, "Bubble oscillations of large amplitude," The Journal of the Acoustical Society of America **68**, 628–633 (1980).
[50]A.-M. Zhang, S.-M. Li, P. Cui, S. Li, and Y.-L. Liu, "A unified theory for bubble dynamics," Physics of Fluids **35**, 033323 (2023).
[51]Q. Wang, K. Yeo, B. Khoo, and K. Lam, "Strong interaction between a buoyancy bubble and a free surface," Theoretical and Computational Fluid Dynamics **8**, 73–88 (1996).
[52]A. M. Zhang and B. Y. Ni, "Three-dimensional boundary integral simulations of motion and deformation of bubbles with viscous effects," Computers & Fluids **92**, 22–33 (2014).
[53]S. J. Lind and T. N. Phillips, "The effect of viscoelasticity on the dynamics of gas bubbles near free surfaces," Physics of Fluids **25**, 022104 (2013).
[54]S. Li and B. Y. Ni, "Simulation on the interaction between multiple bubbles and free surface with viscous effects," Engineering Analysis with Boundary Elements **68**, 63–74 (2016).
[55]B. Y. Ni, A. M. Zhang, and G. X. Wu, "Simulation of a fully submerged bubble bursting through a free surface," European Journal of Mechanics - B/Fluids **55**, 1–14 (2016).
[56]M. J. Miksis, J. M. Vanden Broeck, and J. B. Keller, "Rising bubbles," Journal of Fluid Mechanics **123**, 31–41 (1982).
[57]T. Lundgren and N. Mansour, "Oscillations of drops in zero gravity with weak viscous effects," Journal of Fluid Mechanics **194**, 479–510 (1988).
[58]J. M. Boulton-Stone, "The effect of surfactant on bursting gas bubbles," Journal of Fluid Mechanics **302**, 231–257 (1995).
[59]S. Popinet and S. Zaleski, "Bubble collapse near a solid boundary: a numerical study of the influence of viscosity," Journal of Fluid Mechanics **464**, 137–163 (2002).
[60]Y. L. Liu, A. M. Zhang, Z. L. Tian, and S. P. Wang, "Investigation of free-field underwater explosion with eulerian finite element method," Ocean Engineering **166**, 182–190 (2018).
[61]L. T. Liu, X. L. Yao, N. N. Liu, and F. L. Yu, "Toroidal bubble dynamics near a solid wall at different reynolds number," International Journal of Multiphase Flow **100**, 104–118 (2018).
[62]Y. L. Liu, A. M. Zhang, Z. L. Tian, and S. P. Wang, "Dynamical behavior of an oscillating bubble initially between two liquids," Physics of Fluids **31**, 092111 (2019).
[63]S. Li, Y. Saade, D. van der Meer, and D. Lohse, "Comparison of boundary integral and volume-of-fluid methods for compressible bubble dynamics," International Journal of Multiphase Flow **145**, 103834 (2021).
[64]O. Supponen, D. Obreschkow, P. Kobel, and M. Farhat, "Detailed jet dynamics in a collapsing bubble," Journal of Physics: Conference Series **656**, 012038 (2015).
[65]M. Ivings, D. Causon, and E. Toro, "On riemann solvers for compressible liquids," International Journal for Numerical Methods in Fluids **28**, 395–418 (1998).
[66]Z. L. Tian, Y. L. Liu, A. M. Zhang, and S. P. Wang, "Analysis of breaking and re-closure of a bubble near a free surface based on the eulerian finite element method," Computers & Fluids **170**, 41–52 (2018).
[67]H. Tang, Y. L. Liu, P. Cui, and A. M. Zhang, "Numerical study on the bubble dynamics in a broken confined domain," Journal of Hydrodynamics **32**, 1029–1042 (2020).
[68]Z. L. Tian, Y. L. Liu, A. M. Zhang, L. B. Tao, and L. Chen, "Jet development and impact load of underwater explosion bubble on solid wall," Applied Ocean Research **95**, 102013 (2020).
[69]H. Tang, Z.-L. Tian, X.-Y. Ju, J.-T. Feng, Y.-L. Liu, and A.-M. Zhang, "Experimental and numerical investigations on the explosions nearby a free surface from both sides," Ocean Engineering **278**, 114372 (2023).
[70]D. J. Benson and S. Okazawa, "Contact in a multi-material eulerian finite element formulation," Computer Methods in Applied Mechanics and Engineering **193**, 4277–4298 (2004).
[71]W. T. Liu, A. M. Zhang, X. H. Miao, F. R. Ming, and Y. L. Liu, "Investigation of hydrodynamics of water impact and tail slamming of high-speed water entry with a novel immersed boundary method," Journal of Fluid Mechanics **958**, A42 (2023).
[72]Z. L. Tian, Y. L. Liu, A. M. Zhang, and L. B. Tao, "Energy dissipation of pulsating bubbles in compressible fluids using the eulerian finite-element method," Ocean Engineering **196**, 106714 (2020).
[73]D. J. Benson, "Computational methods in lagrangian and eulerian hydrocodes," Computer Methods in Applied Mechanics and Engineering **99**, 235–394 (1992).
[74]R. Han, A. M. Zhang, S. Tan, and S. Li, "Interaction of cavitation bubbles with the interface of two immiscible fluids on multiple time scales," Journal of Fluid Mechanics **932** (2022).